

Empiquency Representation of Mesh Surface based on Empirical Mode Decomposition

Hsiang-Jen Chien, Chia-Yen Chen

Dept. of Computer Science and Information Engineering
National University of Kaohsiung
Kaohsiung, Taiwan
ayen@nuk.edu.tw

Chi-Fa Chen, Po-Chun Hsueh, Yu-Wei Tseng

Department of Electrical Engineering
I-Shou University
Kaohsiung, Taiwan
cfchen@isu.edu.tw

Abstract—Mesh geometry processing utilities are frequently used in computer graphics applications. In this paper we propose a novel geometry data processing technique that applies a variation of *empirical mode decomposition* (EMD) on mesh surface. Unlike typical frequency-domain techniques that adjust an input signal by separating its frequency components based on predefined basis functions, our work extracts the ingredients of mesh geometry on a signal-driven fashion. The proposed algorithm first parametrizes a closed zero-genus mesh over 2-sphere. In second stage the radii of transformed vertices are decomposed into *intrinsic mode functions* (IMFs) in a mesh-defined topology space. Comparing to many other frequency-domain techniques, our method does not require re-sampling of geometry data, hence no distortion is introduced through the process. In this paper we also show an application of proposed method in surface filtering.

Keywords-digital geometry processing, mesh parametrization, empirical mode decomposition

I. INTRODUCTION

From advances in 3-d reconstruction and computer graphics, mesh processing utilities have been fundamental to many applications. A mesh, or a triangular 2-manifold as it is commonly concerned in the field of graphics, consists of topology and geometry properties. The geometry-related algorithms are designed to work on either spatial or frequency domain. The latter relies on a relatively recent concept of transforming a mesh into its frequency representation, which is usually defined by deriving the Fourier basis or wavelets on a particular 2-manifold. Extending a frequency-domain signal processing technique that is well-developed in 1-dimensional space is, however, not straightforward. Some lossy procedures have to be introduced to “fit” geometry data into a structure where the extension of a traditional method works fine. Fig. 1 demonstrates a lossy geometry resampling procedure which is necessary in many proposed methods. Such a frequency representation is just an approximation of original mesh.

In 1998 Huang et al proposed a new method for analyzing nonlinear and non-stationary signal known as Hilbert-Huang transform (HHT) [1]. Since that proposal the HHT has been widely applied to study the nature of data collected from various sources. It is used to analyze natural phenomenon such as rainfall [2], tides, and temperature trend as well as artificial data such as satellite signal and structural strength of building. The success of HHT is built on the underlying component separation procedure namely *empirical mode decomposition*

(EMD). The procedure results in components termed *intrinsic mode functions* (IMFs) which are well-behaved in Hilbert spectrum for a transformed uni-variate signal. Since EMD extracts these components in an adaptive fashion rather than utilizing any predefined functions (such as cosines and sines as used in Fourier transforms), it is believed that IMFs reflect more physical meanings of signal.

The behavior and use of EMD in higher dimension lead to an unclear field being explored. For multivariate data analysis a generalization is proposed by Rehman et al [3]. For 2-dimensional dataset A. Linderhed has done a series of work on EMD-based image compression techniques [4]. In her work the word *empiquency* is coined to distinguish empirical mode frequency from traditional frequency concept. In [2] the 2-dimensional EMD is further extended to work in spherical topology space. On development of accelerated 2-dimensional EMD procedure [5] demonstrates that the EMD may also work on the Delaunay tessellation of planar domain. Based on these results, we were inspired to invent a mechanism that represents the geometry data in terms of empiquency.

To apply EMD on a mesh surface some problems have to be solved. In the original 1-dimensional EMD the envelops are computed by means of cubic curve fitting algorithm, which is not applicable in higher dimensional space. Besides, triangular 2-manifold may have an arbitrary topology more complicated than \mathbb{R}^1 space. In this paper we propose a lossless algorithm that extracts empiquency components of geometry data from a closed zero-genus mesh surface and requires no resampling.

This paper is organised as follows. In section II a survey of related work is given. In section III the original EMD as well as its 2-dimensional extension are introduced. In section IV we propose a variation of EMD that works on mesh surface. The experimental results are given in section V. In section VI we conclude this paper.

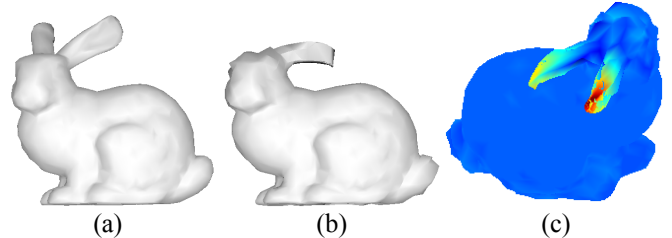


Figure 1. (a) Original and (b) resampled Bunny model and (c) error map

II. RELATED WORK

In early work most of the mesh manipulation tools are developed in rectangular plane space. Mesh parametrization in planar domain has been well studied and become powerful tool in last decade [7]. As planar parametrizations cannot be directly applied to meshes with non-disc topology, some spherical parametrization algorithms have been developed in recent years [8]. These work soon becomes a bridge via which conventional signal processing techniques are turned into mesh processing tools. The spherical harmonics transform (SHT) is such an example. In [9] researchers apply SHT on resampled regular spherical grid of parametrized mesh to remove high-frequency components. The concept then leads to a frequency representation of mesh, which has been used in a wide variety of applications (e.g. [10], [11], and [12]). The SHT is regarded as Fourier transforms of spheres [9]. On the other side, the use of wavelet transforms in similar applications can also be found in literature (e.g. [13]).

Since HHT is frequently compared with Fourier transforms and wavelet transforms in harmonics analysis, researchers are inspired to develop its counterpart in mesh processing. However, there are few work regarding the extension EMD to mesh surface. At the time of writing, we find only one work that attempts to extend EMD in surface fairing application [14]. Similar to aformentioned techniques, the fairing algorithm resamples geometry data over a regular grid. A seperable 2-dimensional EMD algorithm is applied to the matrix representation of resampled radii. By reconstructing signal from smoothed IMFs the high-empiquency noises are filtered. However, we found that the interpolation algorithm in the lossy resampling process also filters out partial noises. It is hard to identify the effort of EMD in reported results.

From a very different perspective namely the spectral graph theory the concept of frequency is described in topology-defined domains, in where spectral approaches need not to solve geometry-related problems such as mesh parametrization and data resampling [15]. These approaches rely on the analysis of eigen-functions of particular Laplacian operator. Due to the computationally diffuculty of finding eigen-decomposition of a massive matrix, these approaches are not practical to deal with meshes consist of hundred thousands of vertices.

III. EMPIRICAL MODE DECOMPOSITION

The EMD is an iterative process that transforms a signal x into linear combination of its intrinsic mode functions (IMFs) h_1, h_2, \dots, h_k and a term of tendency r , as

$$x = h_1 + h_2 + \dots + h_k + r. \quad (1)$$

Unlike Fourier transforms, the decomposition requires only few empiquency components to represent input signal. In following subsections we describe the process of original EMD and its generalization to 2-dimensional Euclidean space.

A. 1-dimensional EMD

The extraction of IMF, which is namely *sifting process* [1], plays an important role of EMD. For an input signal x , the process works as follows:

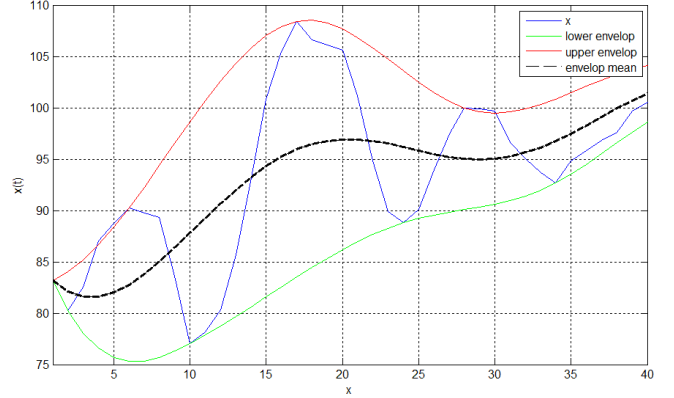


Figure 2. Upper and lower envelops with their mean

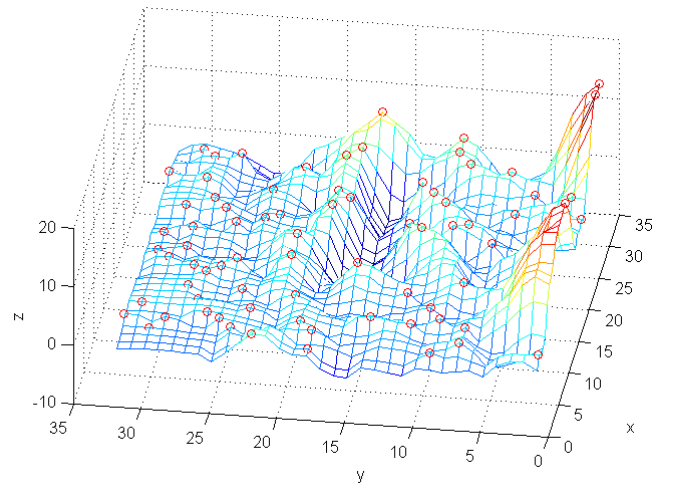


Figure 3. Surface interpolation using Kriging method. The red circles are landmarks referred to compute the interpolation.

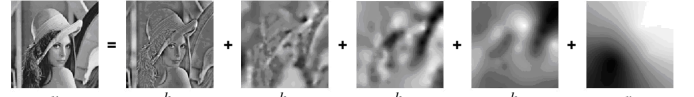


Figure 4. Lena decomposed into four IMFs and the residual.

1. Find local extrema.
2. Perform cubic spline interpolation using local maxima to obtain upper envelop of x , denoted by u .
3. Perform the same interpolation using local minima to obtain lower envelop of x , denoted by l .
4. Subtract the mean of envelops m from input signal, that is to update x by

$$x' = x - m = x - \frac{h + l}{2}. \quad (2)$$

The algorithm of EMD first takes the signal to be analyzed as the input of sifting process, and then repeats the process by passing previously sifted result to next sifting iteration. Such iterative computation stops when convergence criterion are

satisfied. The last output denotes the first IMF h_1 . The extracted component will be subtracted from x , and the rest of x will become the input for the extraction of second IMF h_2 . The extraction of IMF continues until there are no more extrema left in sifted signal. The last remaining indicating the tendency of x is a monotonic component denoted by r , which is called the *residual*. Fig. 2 shows three cubic splines that are calculated during a sifting iteration.

B. 2-dimensional Extension of EMD

Extending EMD to a space higher than one dimension is not trivial. The Fourier transform can be generalized to higher dimensions by applying the transform on each cardinal. Based on a similar concept, some work extend the EMD to image domain by performing 1-dimensional EMD on each row and column respectively (e.g. [14]). The sifted components are combined to yield a 2-dimensional result. However, the EMD generalized in this way does not take the spatial proximity into account and therefore, in our opinion, may lose partial physical meanings.

To apply EMD in 2-dimensional Euclidean space, the sifting procedure needs modification. Recall that the procedure seeks for the extrema to compute envelopes. It is intuitive to locate extrema in 2-dimensional data by means of the eight-neighbor topology. However, computing upper and lower envelops, which is a surface fitting problem in 2-dimensional space, requires more sophisticated interpolation algorithm. In literature the thin-plate spline and radial-basis functions are found to be good solutions. In our work the Kriging interpolation [2] is implemented. For n landmarks the interpolation involves solving a linear system with $n+1$ equations. The interpolant at location (x, y) is given by

$$\hat{f}(x, y) = \begin{bmatrix} Z_{n \times 1} \\ 0 \end{bmatrix}^T \begin{bmatrix} D_{n \times n} & I_{n \times 1} \\ I_{1 \times n} & 0 \end{bmatrix}^{-1} \begin{bmatrix} E_{n \times 1} \\ 1 \end{bmatrix}, \quad (3)$$

where Z contains values of n extrema, D is the mutual distance matrix of extrema, and E denotes the distances between (x, y) to each extrema. Left two matrices are irrelevant to the location of interpolant and can be computed in advance.

Fig. 3 illustrates a solution to surface fitting problem acquired by Kriging method. The decomposition of an image using 2-dimensional EMD is shown in Fig. 4.

IV. EMPIRICAL MODE DECOMPOSITION OF MESH SURFACE

A. Overall Strategy

The proposed algorithm decomposes geometry data of a mesh through two stages. In first stage the geometry of mesh is mapped onto a spherical triangular mesh. This process is known as spherical parametrization. In second stage the geometry is converted to spherical coordinate system and the radii are projected onto vertices. The mapped geometry data are then decomposed into empirical components using a modified sifting procedure. Because geometry data are processed in spherical domain, our method is rotation-invariant and scale-invariant. Beside, through the process no distortion of geometry is introduced because our method does not require the spherical signal to be resampled on regular grid.

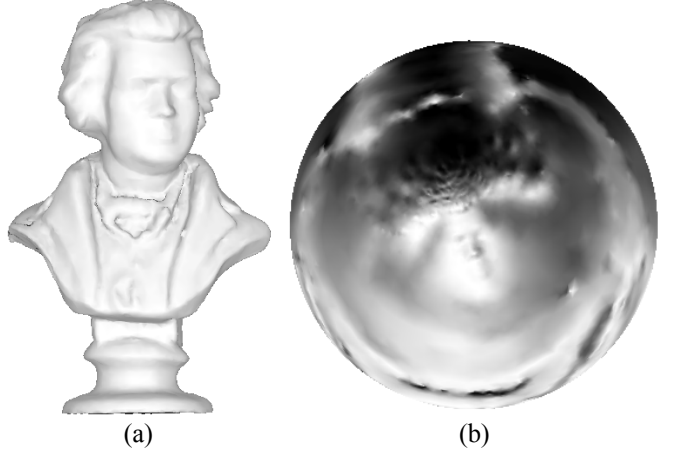


Figure 5. Model MOZART and its spherical parametrization. The center of sphere maps to the facial region.

B. Spherical Parametrization

A closed zero-genus triangular mesh is an embedding of 2-manifold in 3-dimensional Euclidean space [8]. According to the well-known Steinitz's theorem such mesh is a deformed sphere. In other words, this kind of meshes is topologically equivalent to the unit sphere S^2 and we can always find a valid embedding. Unfortunately, despite the theorem guarantees the existence of spherical parametrization, there exist infinitely many embeddings for a 2-manifold mesh.

In last decade numerous solutions were proposed to address the spherical parametrization problem. The philosophies of these methods differ in the definition of distortion being minimised. The preserved properties include angle (conformal map), area of triangle (equi-area map), harmonic energy[16], Tutte energy [8], stretch energy, etc. Among proposed methods only few of them are practical to deal with large complicated meshes, which are generally consist of hundred thousands of vertices [18]. In our work the spherical embedding is found by an efficient iterative computation scheme. More specifically it is a Gauss-Seidel process that repetitively relaxes vertex positions on the sphere. Given G_i the $m \times 3$ geometry matrix of i -th iteration and $\eta \in (0, 1]$ the damping parameter, the updating rule is

$$G'_{i+1} = (1 - \eta) G_i + \eta L G_i, \quad (4)$$

where L is a kind of Laplacian operator which is denoted by a $m \times m$ matrix

$$l_{i,j} = \begin{cases} \frac{1}{\|adj(v_i)\|} & , v_j \in adj(v_i) \\ 0 & , otherwise \end{cases}. \quad (5)$$

Equation (4) and (5) can be combined into a Laplacian operator

$$l_{i,j} = \begin{cases} 1 - \eta & , v_i = v_j \\ \frac{\eta}{\|adj(v_i)\|} & , v_j \in adj(v_i) \\ 0 & , otherwise \end{cases}. \quad (6)$$

The definition of L depends on the property we desire to preserve under the mapping. In our case the solver approaches

a local optimal solution of the boundary-free spring energy minimisation problem. In the experiment we found that without proper stopping criteria the scheme will eventually reach global optimum - the trivial solution that collapses all vertices to one point. To avoid such situation we track the change of system and stop when the change becomes insignificant. Note we need to apply the normalisation $G_{i+1} = G'_{i+1} / \|G'_{i+1}\|$ after each update to fix updated vertex positions on the unit sphere. Fig. 5 shows a mesh and its spherical parametrization obtained after hundreds of iterations.

C. Sifting of Spherical Signal

To perform sifting procedure we need to define local extrema of a surface. In this work the extrema are found by means of mesh topology. More specifically, a vertex is said to be a extremum if associated value is larger or smaller than any of its connected vertices. The measure of distance between two vertices is defined as great circle distance on 2-sphere. Since we have chosen the unit sphere as parametrization domain, the distance of any two connected vertices u, v is simply the arccosine

$$\delta(u, v) = \arccos(u \cdot v). \quad (7)$$

Based on the definition of extrema and distance function, we use equation (7) to compute envelopes by means of Kriging interpolation. The mean of upper and lower envelopes is subtracted to produce a sifted signal. This procedure repeats until standard deviation of mean envelop becomes significantly small.

V. EXPERIMENTAL RESULT

To demonstrate proposed algorithm we decomposed a scan of Mozart statue, which is a zero-genus surface containing more than 25,000 vertices, into its empirical components. The maximal number of sifting iteration is set to 100. The stopping criterion is reached when the root-mean-square of changes of vertex data is evaluated less than 0.01. We extracted first 11 IMFs from the mesh surface. Fig 6 shows the resulting components in parameter domain. To properly visualise extracted components in Euclidean space, the residual is added to each IMF. The results are listed in Fig. 7. In Fig. 8 the original geometry data is progressively reconstructed in Euclidean space by adding IMFs one by one to the residual.

We also provide an example to show the proposed method can be used to achieve feature-preserve surface filtering. The geometry data shown in Fig. 9 is reconstructed from IMFs with first 6 components filtered by a Laplacian operator, which is also applied to original mesh as shown in fig. 10. These results show that by applying frequency-domain operator on partial IMFs a surface is smoothed without much loss of its detail.

VI. CONCLUSION AND FUTURE WORK

In this paper a variation of 2-dimensional EMD is proposed to extract geometrical empirical components of a mesh. Comparing to other work, proposed method does not perform resampling of geometry data, hence no distortion is introduced

in the empirical representation. In future work we will study how different parametrization techniques affect the result of decomposition. We will also explore more usages of proposed mesh representation on next step.

ACKNOWLEDGEMENT

This research was sponsored by National Science Council of Taiwan under grant number NSC 99-2221-E-214-064.

REFERENCES

- [1] N. E. Huang et al, "The empirical mode decomposition and the Hilbert spectrum for nonlinear and non-stationary time series analysis," Proc. R. Soc. Lond. A, vol. 454, no. 1971, pp. 903–995, 8 March 1998.
- [2] G. Sinclair, and G. S. Pegram, "Empirical Mode Decomposition in 2-D space and time: a tool for space-time rainfall analysis and nowcasting," J. Hydrology and Earth System Sciences, vol. 9, pp. 127–137, 2005.
- [3] N. Rehman and D. P. Mandic, "Multivariate empirical mode decomposition," Proc. Royal Society A, vol. 466, no. 2117, pp. 1291–1302, 2010.
- [4] A. Linderhed, "Variable sampling of the Empirical Mode Decomposition of two-dimensional signals," J. Wavelets, Multiresolution and Information Processing, vol. 3, pp. 435–452, 2005.
- [5] Y. Xu, B. Liu, J. Liu and S. Riemenschneider, "Two-dimensional empirical mode decomposition by finite elements," Proc. Royal Society A, vol. 462, no. 2074, pp. 3081–3096, 2006
- [6] Z. Yang, D. Qi, and L. Yang, "Signal period analysis based on Hilbert–Huang transform and its application to texture analysis," Proc. International Conference on Image and Graphics, pp. 430–433, 2004.
- [7] A. Sheffer, E. Praun, and K. Rose, "Mesh parameterization methods and their applications," Foundations and Trends in Computer Graphics and Vision, vol. 2, pp. 105–171, 2006.
- [8] C. Gotsman, X. Gu, and A. Sheffer, "Fundamentals of spherical parameterization for 3D meshes," ACM Transactions on Graphics, vol. 22, pp. 358–364, 2003.
- [9] K. Zhou, H. Bao, and J. Shi, "3D surface filtering using spherical harmonics," J. Computer-Aided Design, vol. 36, pp. 363–375, 2004.
- [10] L. Li, D. Zhang, Z. Pan, J. Shi, K. Zhou, and K. Ye, "Watermarking 3D mesh by spherical parameterization," Computers and Graphics, vol. 28, pp. 981–989, 2004.
- [11] M. Mousa, R. Chaine, and S. Akkouche, "Frequency-based Representation of 3D Models using Spherical Harmonics," Proc. WSCG'06, pp. 193–200, 2006.
- [12] M.H. Mousa, R. Chaine, S. Akkouche, and E. Galin, "Efficient Spherical Harmonics Representation of 3D Objects," Proc. 15th Pacific Conference on Computer Graphics and Applications, pp. 248–255, 2007.
- [13] A. Jalobeanu, "Fractal 3D Modeling of Asteroids using Wavelets on Arbitrary Meshes," Proc. of IAFRA'03, 2003.
- [14] X. Qin, X. Chen, S. Zhang, and W. Wang, "EMD Based Fairing Algorithm for Mesh Surface," Computer-Aided Design and Computer Graphics, pp. 606–609, 2009.
- [15] B. Lévy, H. Zhang, "Spectral Mesh Processing," Proc. SIGGRAPH'10 Computer Graphics Forum, vol. 29, pp. 1865–1894, 2010.
- [16] X. Gu, Y. Wang, F. Chan, P.M. Thompson, and S.T. Yau, "Genus Zero Surface Conformal Mapping and Its Application to Brain Surface Mapping," Trans. on Medical Imaging 2004, vol. 23, pp. 949–958, 2004.
- [17] I. Friedel, P. Schröder, and M. Desbrun, "Unconstrained Spherical Parameterization," Proc. SIGGRAPH'05 Sketches, vol. 12, pp. 134–142, 2005.
- [18] S. Saba, I. Yavneh, C. Gotsman, and A. Sheffer, "Practical spherical embedding of manifold triangle meshes," Proc. International Conference on Shape Modeling and Applications, pp. 256–265, 2005.

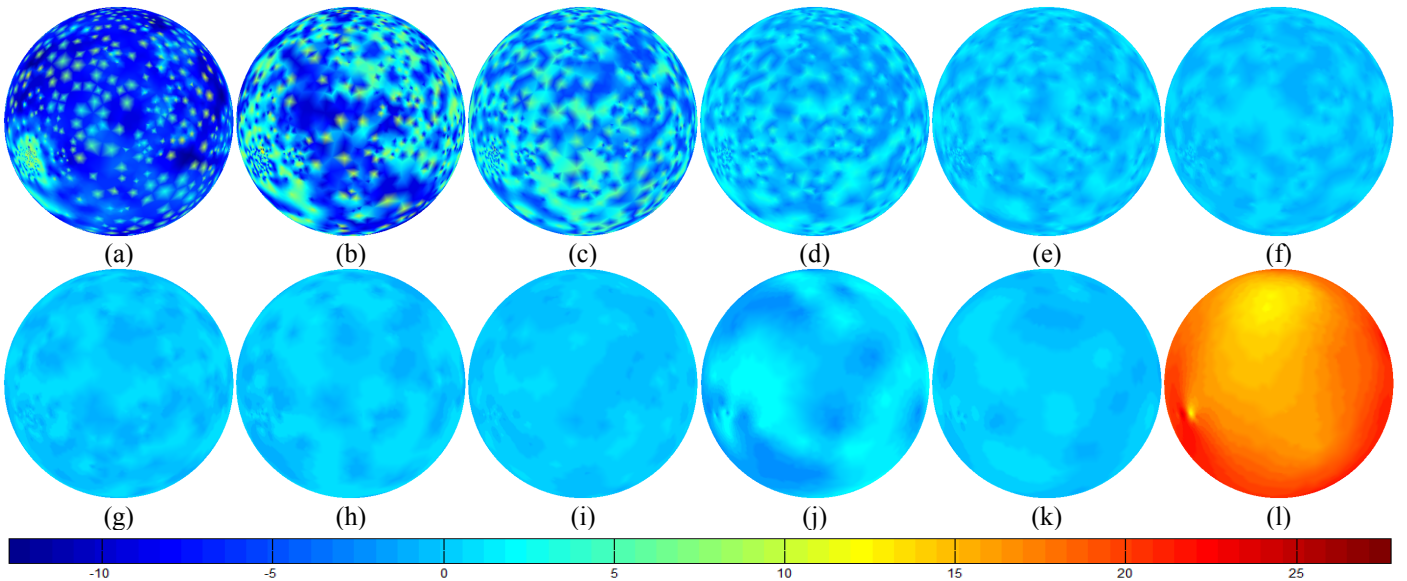


Figure 6. Colour-coded visualisation of (a)-(k) first 11 IMFs and (l) the residual trend of mesh Mozart

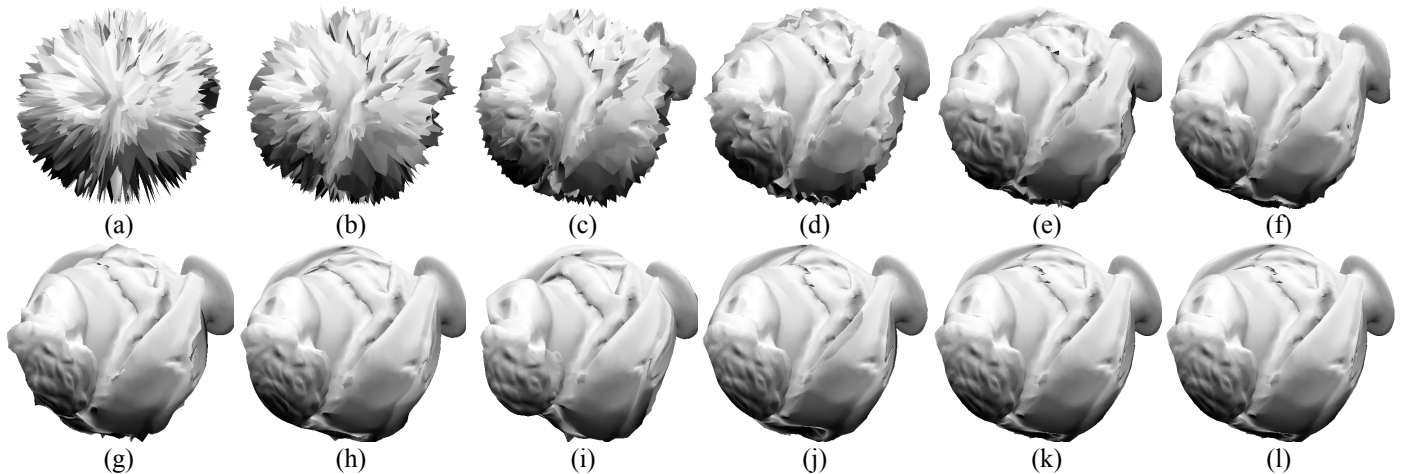


Figure 7. Visualisation of (a)-(k) first 11 IMFs and the (l) residual trend in Euclidean space

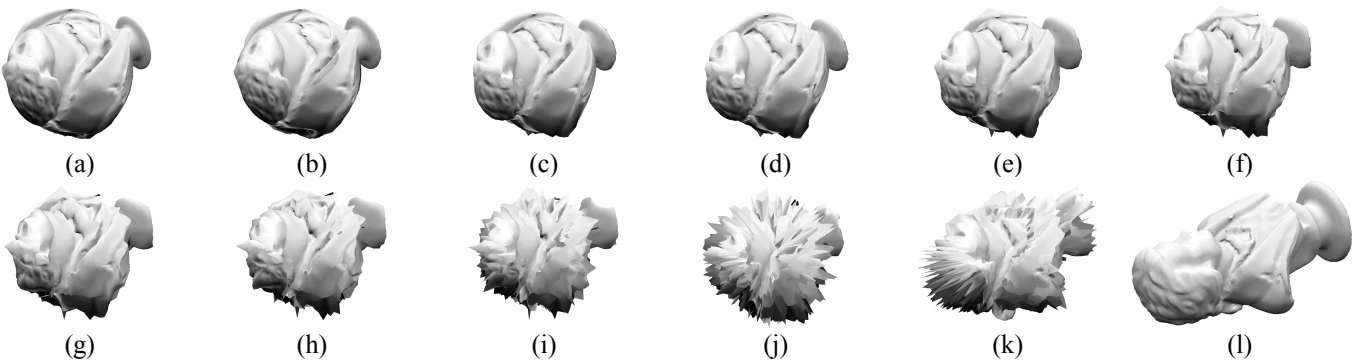


Figure 8. Reconstruction of mesh geometry from (a) the base through (b) 11th IMF to (l) 1st IMF



Figure. 9. Mozart smoothed by applying a Laplacian operator on first 6 IMFs



Figure. 10. Mozart smoothed by applying the same operator on mesh geometry data